Journal of Membrane Science & Research

journal homepage: www.msrjournal.com

Research Paper

Study on commercial membranes and sweeping gas membrane distillation for concentrating of glucose syrup

Mohammad Mahdi A. Shirazi [1,2,†], Ali Kargari [3,*], Dariush Bastani [4], Mansooreh Soleimani [5], Leila Fatehi [2]

[1] *Membrane Industry Development Institute, Tehran, Iran*
[2] *Department of Chemical Engineering, Faculty of Petroleum and Chemical Engineering, Science and Research Branch, Islamic Azad University, Tehran, Iran.*
[3] *Membrane Processes Research Laboratory (MPRL), Department of Chemical Engineering, Amirkabir University of Technology (Tehran Polytechnic), Tehran, Iran.*
[4] *Department of Chemical and Petroleum Engineering, Sharif University of Technology, Tehran, Iran.*
[5] *Department of Chemical Engineering, Amirkabir University of Technology (Tehran Polytechnic), Tehran, Iran.*

Article info

Received 2019-03-30
Revised 2019-08-26
Accepted 2019-08-27
Available online 2019-08-28

Keywords

Sweeping gas membrane distillation
SGMD
Glucose syrup
3HUPHDWH ÀX[
Membrane performance
Module design

Highlights

- SGMD process opportunities applied to bioethanol process.
- Investigating three commercial membranes made of PP, PVDF and PTFE.
- 6WXG\ RQ WKH HuHFW RI ÀRZ DUUDQJHPHQWV DQG PRGXOH GHVLJQ
- ,QWURGXFLQJ WKH FURVV FXUUHQW ÀRZ DV D QHZ PRGXOH GHVLJQ IRU SGMD process.

Graphical abstract

Abstract

In this work, sweeping gas membrane distillation (SGMD) process was used for concentrating of glucose syrup. The main questions in this work include: is SGMD process practic
IRU FRQFHQWUDWLQJ RI JOXFRVH VROXWLRQ SULRU WKH IHUPHQWDWLRQ VWHS LQ ELRHWKDQRO SURF
the SGMD process in pilot scale for this issue?. To answer these questions, SGMD process was performed using three commercial membranes made of PP, PVDF and PTFE
membranes characterized using scanning electron and atomic force microscopes for their morphological and topographical features. Important operating parameters including fe
temperature (45-65 °C), IHHG ÀRZ UDWH (... P/ PLQ) IHHG FRQFHQWUDWLRQ ... ZHUH LQYHVWLJDWHG DV IRU WKHLU HuHFWV RQ ...
ÀX[DQG WKH RSWLPL]HG SDUDPHWHUV ZHUH WKHQ UHSRUWHG. 0RUHRYHU, WKH LQÀXHQFH RI WKUHH ...
SHUPHDWH ÀX[ZDV VWXGLHG. 7KH EHVW SHUIRUPDQFH, WKH KLJKHVW SHUPHDWH ÀX[DQG UHMHFWLRQ ...
conditions (feed temperature: 65 °C, IHHG ÀRZ UDWH ... P/ PLQ, ... JOXFRVH, ÀRZ DUUDQJHPHQW: FKDQQHO PRGHO, ... PP DQG WKH FURVV ...
indicated that SGMD process is a promising option for concentrating of the sugar syrup prior the fermentation step in the bioethanol production process.

1. Introduction

As time goes by, liquid biofuels as one of the most sustainable energy sources has been attracted a lot of attention, globally. Bioethanol has DGYDQWDJH LQ GLUHFW PL[LQJ ZLWK FRQYHQWLRQDO petro-diesel in order to decrease the air pollution problems [1,2]. Among other clean and renewable biofuels, bioethanol has gained more attention due to its various and interesting advantages. It can be produced from a wide range of ELRPDVV DQG FDQ EH ... [3,4] PL[HG E\ JDVROLQ... The Every bioethanol production include biomass harvesting, grinding, and pretreatment, and it then will follow by fermentation and ethanol recovery steps as the process major parts [5-8]. Most of these production stages need large amount of input energy, either in steam or electricity forms, as well as large amount of steels for equipment. Therefore, the bioethanol will not be a

&RUUHVSRQGLQJ DXWKRU DW 3KRQH ... ID[...
E-mail address: kargari@aut.ac.ir and ali_kargari@yahoo.com (A. Kargari)

DOI: 10.22079/JMSR.2019.105700.1257

promising option without significant improvements in production process, energy consumption and equipment design. In this regard, membrane separation technology can integrate the bioethanol process in order to intensification and economization of production, especially into two major steps, i.e. concentration of dilute sugar syrup in prehydrolyzates prior to fermentation step and ethanol recovery either during or after fermentation process [9, 10].

Further to ethanol recovery after the fermentation step, membrane technology can effectively be used for concentrating of simple sugar syrup prior to fermentation step. It is to be noted that low concentration of simple sugar in prehydrolyzates, due to the different pretreatment processes and hydrolysis efficiency, can lead to low ethanol concentration. It can be translated to higher production cost and energy demand for subsequent biorefinery (i.e. purification step) [9, 10]. Therefore, in order to enhance the productiveness of fermentation process, a concentrating step is necessary to increase the concentration of the sugar in the syrup before the fermentation process.

The well-developed techniques for concentrating of sugar syrups include evaporation, nanofiltration (NF) and reverse osmosis (RO) [9, 11, 12]. However, it should be noted that these methods have some disadvantages such as high operating cost, high energy consumption, water recovery limitation (i.e., osmotic pressure limitation for NF and RO processes), generating additional waste, long operation time and wasting sugars [13]. A new hybrid, non-isothermal membrane process has been nominated which is an amalgamation of membrane separation and the traditional distillation processes, which is called “Membrane Distillation” [14]. In spite of the fact that this process has been introduced for five decades, it still requires to be studied and developed, especially for new applications and pilot scales.

The membrane distillation (MD) process uses the vapor-pressure difference as the driving force. The temperature difference between the two sides of a hydrophobic microporous membrane provides the corresponding vapor-pressure [15]. This process, not only portions out the unique specifications of the membrane processes, but can also be driven by renewable energy sources. The MD process has four major configurations depending on the design of the permeate side including DCMD (direct contact membrane distillation), SGMD (sweeping gas membrane distillation), AGMD (air-gap membrane distillation), and VMD (vacuum membrane distillation) processes. The feed side (i.e., hot stream) in all these configurations is the same. However, the changes are made on the permeate side for setting up the driving force. In the SGMD process, an inert gas sweeps the permeated vapor molecules in the cold side. The SGMD process has some highlighted merits over other MD configurations including comparatively lower conductive heat loss through the membrane bulk and lessened mass transfer resistance. In contrast of the AGMD process that the gas-gap dramatically imposes a serious resistance against the permeation of vapor molecules and consequently decreases the permeate flux, the gas in SGMD is not immobile and collects the vapor molecules from the membrane surface. This can result in higher mass transfer through the membrane pores and consequently provides higher permeate flux in SGMD. Moreover, the SGMD process is more practical than that of the DCMD process for removal of organic materials from aqueous solutions. This attributes to the considerably lower pore wetting risk of the applied membrane from the permeate channel [15-17].

In this work, we try to investigate some niches of SGMD process opportunities applied to bioethanol production: is SGMD process practical for concentrating of sugar syrup prior the fermentation step of bioethanol process?; are the commercially available hydrophobic membranes sufficient enough to scaleup the SGMD process for concentrating of sugar syrup, and if not what are the expected improvement? Therefore, three commercial hydrophobic membranes with same pore sizes, and various thicknesses were used for concentrating of glucose syrup using the SGMD process. The effect of pertinent operating parameters was studied and discussed, comprehensively. Moreover, a new configuration for flow arrangement in SGMD module was introduced and tested.

2. Experimental

2.1. Materials

Glucose with analytical grade (purity > 99.4%; Merck) and distilled water were used for preparation of feed samples with the desired concentrations (10-50 g/L). Dry air (after filtration) was used as the sweeping gas (vapor carrier in the permeate side). Commercial flat sheet hydrophobic membranes PVDF (polyvinylidene fluoride), PP (polypropylene) and PTFE (polytetrafluoroethylene) were used in experiments. Table 1 presents the features of the applied membranes, as reported by suppliers.

2.2. Experimental set-up and procedure

A SGMD apparatus with a membrane active area of ~170 cm^2 was used for the experiments. A flat sheet membrane was located in a horizontally mounted plate-and-frame module made of Plexiglas TM. Figure 1 shows a general scheme of the experimental setup. In all experiments, the active layer of the membranes was faced up to the hot feed stream. The tangential flow pattern was established in the module for the hot stream using a diaphragm pump. Three different flow arrangements were investigated, including co-current, counter-current and cross-current (see Figure 2). In all flow arrangements, the hot feed flows in from the bottom side of the membrane while the condensing liquid flows in from the top side of the module. The effect of superficial velocity on the permeation rate was studied by changing the depth of feed and permeate channels.

The sweeping gas flow was provided by an oil-free compressor (GAST, USA). A water bath equipped with a liquid circulator and a PID controller was used for adjusting the feed temperature. Thermal sensors were placed on the inlet and outlet points of the membrane module for temperature measurement. A jacketed graduated glass vessel was used as the feed tank and was equipped with an agitator and a temperature sensor for monitoring and controlling the feed stream temperature. Feed and sweeping gas flow rates were adjusted by two precise flow meters in the range of 400-800 mL/min for the liquid-feed stream and 0.113-0.453 Nm^3/h for the sweeping gas stream, respectively.

All experiments were conducted for 240 min. In this work, the permeate flux was considered as the target parameter, and reported values for flux are the average values. Moreover, the concentration of glucose in feed and permeate streams were also measured.

2.3. Analysis

The concentration of glucose was measured in feed and permeate streams every 30 min by the glucose-oxidase colorimetric method [18]. The permeate flux measurement for the conducted experiments was described in the previous study [19].

Membranes’ morphology was observed by scanning electron microscopy (SEM) (VEGA, TESCAN). A contact angle measuring system (KRUSS G-10, Germany) was used for testing the hydrophobicity of the membranes. Topographical observation of the applied membranes was carried out using the atomic force microscopy (AFM) analysis (DUALSCOPE 95-200E, Denmark). SEM and AFM images of the membranes with 0.22 µm pore size are shown in Figure 3. Detailed information of the AFM characterization procedure can be found in the previous works [20-22].

2.4. Experimental design

It is evidently necessary to identify the most effective process parameters for optimizing the SGMD process. The target parameter in this study is the permeate flux. Classical methods for process design have the demerit of complexity. Moreover, they are not easy to use and a large number of tests have to be conducted, especially when the number of process variables is large.

Taguchi method is one of the most practical optimization methods, which has widely been used for experimental design for sensitivity analysis studies [23, 24]. The Taguchi method uses orthogonal arrays with a special design to investigate the effect of process parameters with only a few number of experiments [25]. Thus, the Taguchi experimental design was used for optimization of operating parameters in this work. One of the positive features of this method is the capability in determining the influence and contribution of each variable in the final response. Based on the Taguchi design methodology, four variables in three levels (an L_9 orthogonal array) was considered. Table 2 represents the experimental variables, their levels and the results obtained by use of each membrane.

Table 1
The properties of the membranes used in the present study, reported by suppliers.

Material	Pore size (µm)	Support	Thickness (µm)	Supplier
PTFE	0.22	PP fibers	175	Millipore
PP	0.22	Un-supported	200	Membrane-Solution
PVDF	0.22	Non-woven	184	Sepro

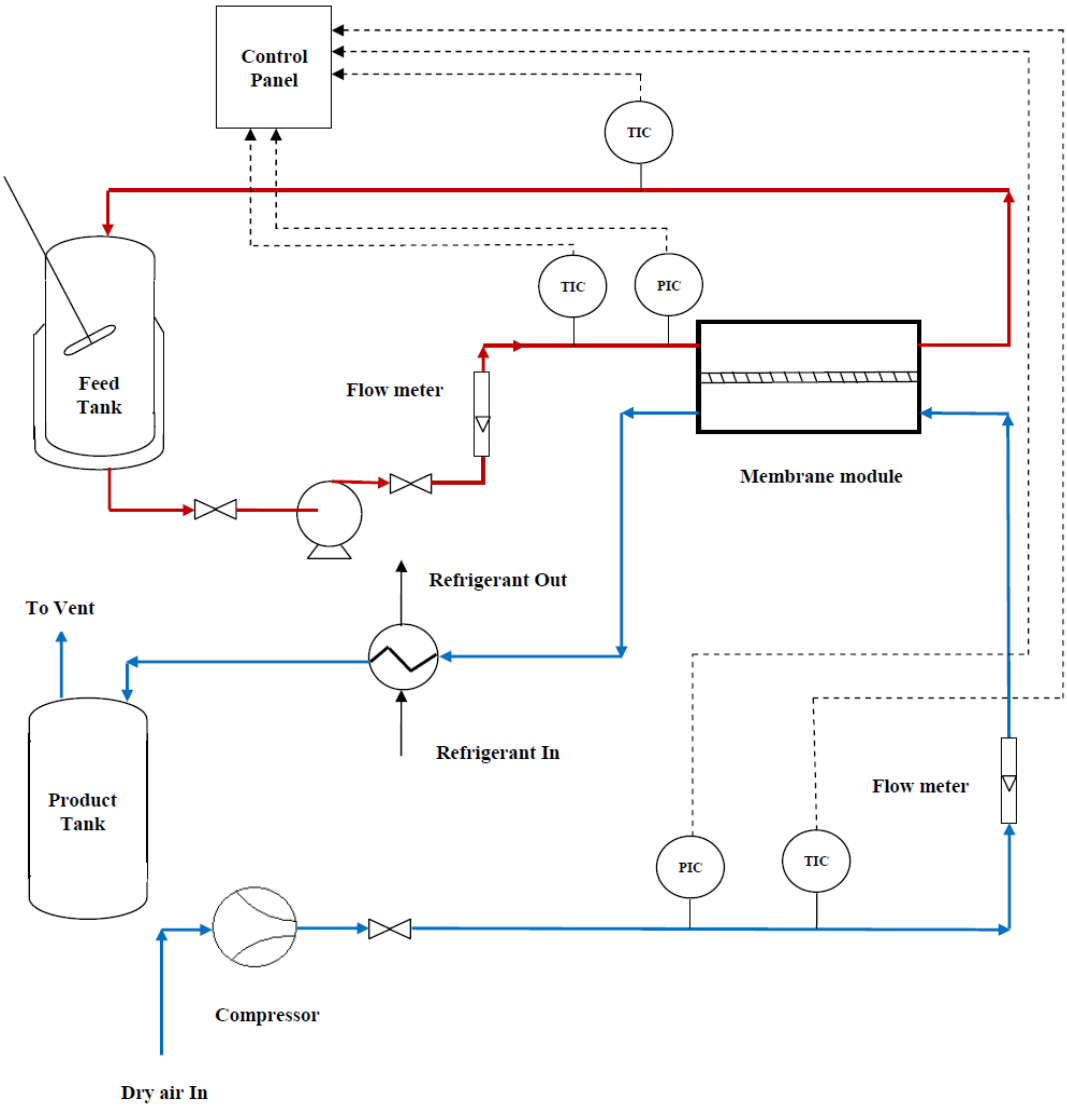

Fig. 1. The general scheme of the experimental set-up.

Table 2
Operating variables (T_h: °C; Q_h: mL/min; C_i: kg/m^3; Q_s: Nm^3/h) and their levels based on the Taguchi L_9 orthogonal array, and the experimental permeate flux (L/m^2.h) for each membrane (PTFE, PVDF and PP, respectively).

Run No.	T_h	Q_h	C_i	Q_s	PTFE	PVDF	PP
1	45	400	10	0.113	5.03	4.8	4.21
2	45	600	30	0.283	5.37	5.1	4.82
3	45	800	50	0.453	6.64	5.31	4.78
4	55	400	30	0.453	7.38	6.7	4.42
5	55	600	50	0.113	6.20	4.9	3.43
6	55	800	10	0.283	8.80	5.45	5.32
7	65	400	50	0.283	8.10	7.21	5.76
8	65	600	10	0.453	15.39	12.78	10.21
9	65	800	30	0.113	10.54	9.77	8.22

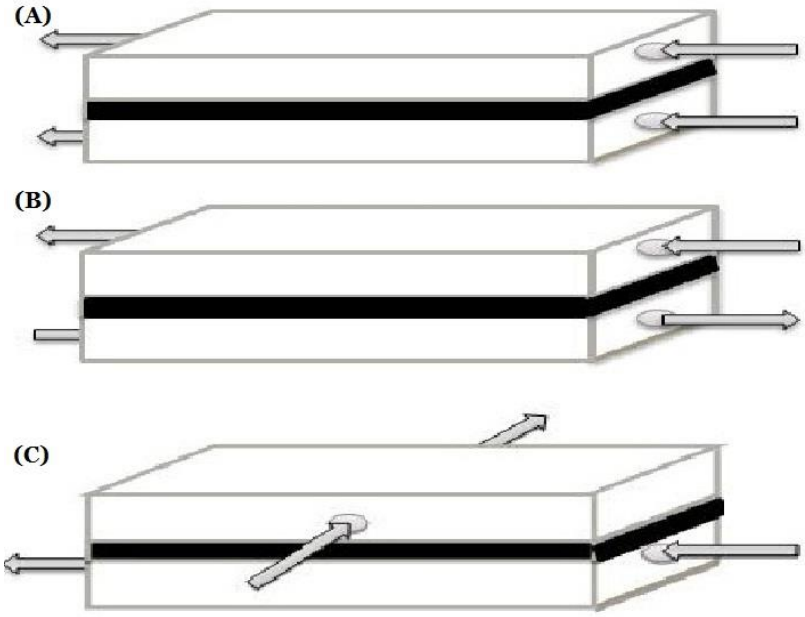

Fig.2. Flow arrangements for the hot and cold streams; (a) co-current, (b) counter-current and (c) cross- current.

3. Results and discussion

3.1. Main effects of feed temperature

As mentioned earlier, the MD process uses the vapor-pressure difference, which is imposed by temperature difference between the feed and the permeate channels as the driving force. In the present study, three feed temperatures of 45, 55 and 65°C were investigated to study the SGMD permeate flux variation.

According to the well-known Antoine equation, the vapor pressure of a saturated pure liquid increases exponentially with the temperature [26]. Therefore, as the feed temperature increases, the change in partial vapor-pressure becomes more. Thus, more vapor molecules can pass through the membrane pores. This can be attributed to the higher permeate flux when higher range of feed temperature is imposed. For instance, about 0.1°C temperature drop at 30°C can result in about 24.4 Pa variation in the vapor-pressure, whereas at 70°C, the same values changes by 135 Pa [27].

Figure 4 shows that for all membranes, the permeate flux increases by using higher range of the feed temperature. The PTFE membrane provided higher permeate flux in comparison with the PVDF and PP membranes. This can be attributed to the lower surface energy and thinner structure of the PTFE membrane compared with other two membranes. At higher feed temperatures, the mass transfer resistance is lower for a more hydrophobic and thinner membrane. In better words, higher hydrophobicity and less thickness can be translated to higher liquid entry pressure and shorter mass transfer length, respectively, in which both mean higher permeate flux production.

On the other hand, higher permeate flux was provided for by using the PVDF membrane as compared with the PP membrane (see Figure 4). This could be explained as follow. As it stated earlier, the membrane thickness is one of the effective parameters on the permeate flux. Higher mass transfer resistance is expected for thicker membranes [15]. As could be observed in Table 1, the thicknesses of PTFE, PVDF and PP membranes are 175, 184 and 200 µm, respectively. Therefore, it could be concluded that lower and higher thicknesses of the PTFE and PP membranes have contributed to their higher and lower permeate flux at higher operating temperature, respectively. However, it is indicated in the literature that thicker membranes can perform better when high concentration of solute(s) is imposed to the feed stream [28].

On the other hand, the permeate flux increased for both the PVDF and PTFE membranes with increasing the feed temperature up to 65°C. However, using the PP membrane the permeate flux slightly decreased up to 55°C and then increased up to 65°C. This result can be attributed to the effect of the membrane thickness. When low operating temperature introduces to a thick membrane, in this case the PP membrane with 200 µm thickness, lower permeate flux will be achieved due to higher mass transfer resistance for transferring the vapor molecules through the pores. However, higher operating temperature can provide higher permeate flux by using thick membranes [29]. In better words, the polarization effects can affect less significant for thicker membranes at high feed temperatures (see Figure 4).

Higher feed temperatures in the SGMD process can amplify the effect of the temperature polarization [30]. As could be observed in Figure 3, the PP membrane structure (which was made through the melt-spinning method) contains randomly formed fibers without any support layer. One may ask about the effect of the basic polymer (PP, PVDF or PTFE) and the structure (fibrous or 2D dimensional) on the membrane performance (see Figure 4). The proposed structures can lead to increase the polarization effect when these membranes, which are specifically fabricated for microfiltration purposes, applied for the MD process. In contrast, the thinner PTFE and PVDF membranes, which are made through stretching and phase-inversion methods, respectively, and consist a two-dimension composite structure including a support layer and an active hydrophobic layer, showed better performance at lower operating temperatures, which can be attributed to their lower temperature polarization effect.

It is comprehensively discussed in the literature that higher operating temperature can provide more vapor molecules in the permeate channel which means higher productivity [15,31,32]. As could be observed, the higher range of feed temperature (55 to 65°C) provided more permeate flux than that of the lower range (45 to 55°C). However, it is to be noted that the energy consumption to provide the latent heat in the lower temperature ranges (i.e. 45-55°C) could be higher than that of higher temperature ranges (i.e. 55-65°C). Therefore, using low grade and/or waste energy sources which can be available in industry can be investigated as a strategy for economizing the SGMD process [33]. Moreover, solar energy, as another alternative and renewable energy source, which is widely available in arid regions like the Middle East [34,35] can effectively be used to set up solar-assisted SGMD pilots.

As mentioned earlier, a comparison between the applied membranes with the 0.22 µm pore size shows that the PTFE membrane resulted in higher permeate flux (see Table 2). Table 3 shows the results of the experimental runs and the corresponding energy consumptions based on the Taguchi experimental design for the PTFE membrane. As could be observed, the higher permeate flux was obtained when the feed temperature of 65°C and the feed concentration of 10 g/L were used (i.e. the run 8), and the corresponding energy consumption was about 2.22 kWh.

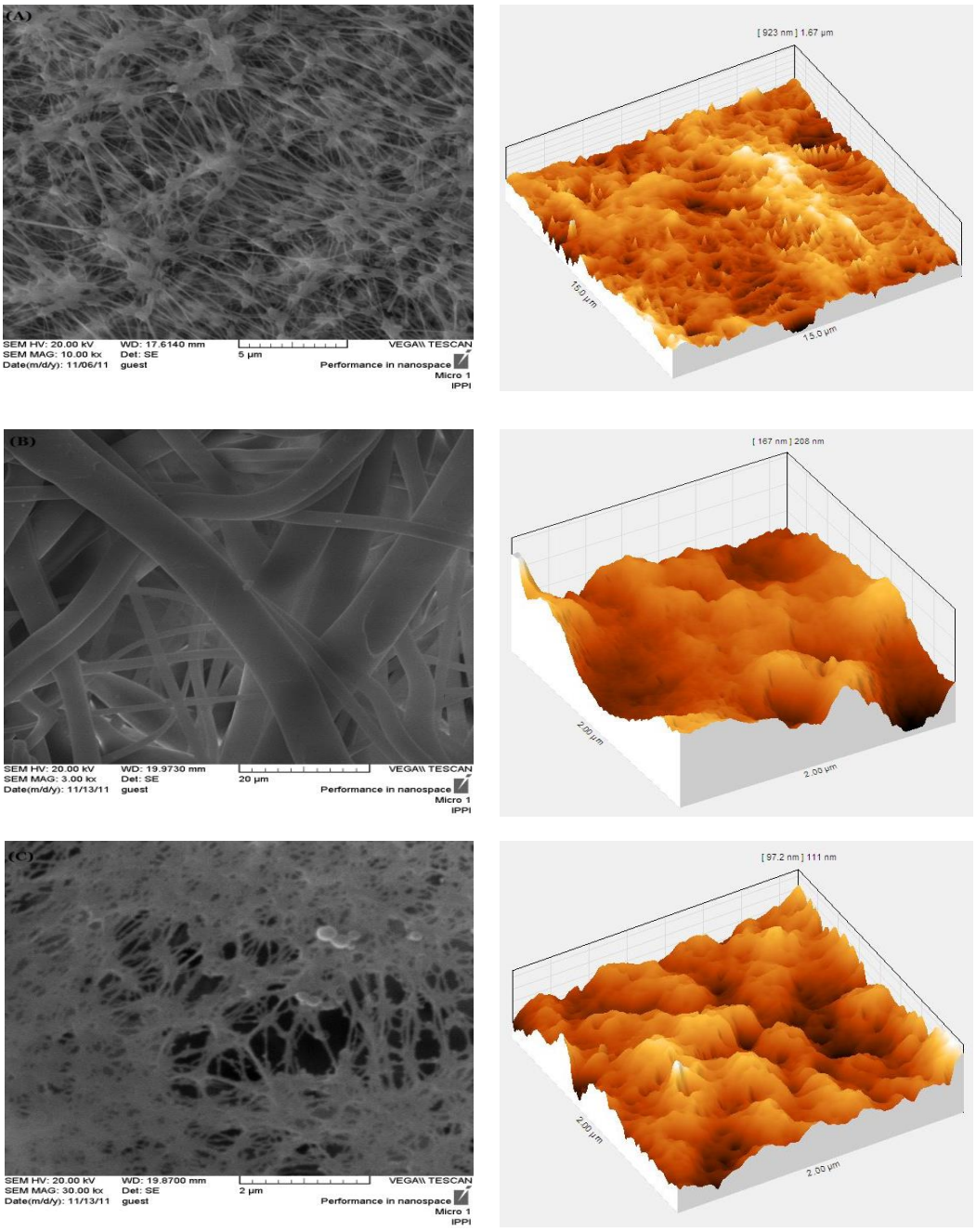

Fig.3. SEM (left) and AFM (right) images of (A) PTFE, (B) PP and (C) PVDF membranes with 0.22 µm pore size.

Table 3
The results of the experiments based on the Taguchi experimental design for the PTFE membrane with 0.22 µm pore size.

Run No.	T_h	Q_h	C_i	Q_s	Flux (L/m^2.h)	C_i	C_f	S (%)	E (kWh)
1	45	400	10	0.113	5.03	10	14.88	48.8	0.97
2	45	600	30	0.283	5.37	30	45.64	52.1	0.31
3	45	800	50	0.453	6.64	50	82.25	64.5	0.40
4	55	400	30	0.453	7.38	30	51.50	71.6	1.47
5	55	600	50	0.113	6.20	50	80.11	60.2	2.12
6	55	800	10	0.283	8.80	10	18.54	85.4	1.35
7	65	400	50	0.283	8.10	50	89.33	78.6	2.18
8	65	600	10	0.453	15.39	10	20.94	109.4	2.22
9	65	800	30	0.113	10.54	30	56.79	89.3	3.49

T_h: ^oC
Q_h: mL/min
C_i and C_f: kg/m^3
Qs: Nm^3/h
S (%): percentage of separation in each run

Table 4
The reported and the measured specifications of applied membranes.

Membrane	Reported			Measured		
	Pore size (µm)	Thickness (µm)	Porosity (%)	Pore size (µm)	Roughness (nm)	CA (º)
PVDF	0.22	184	80	0.311	11.9	98.7
PP	0.2	200	75	0.282	51.7	113.5
PTFE	0.22	175	70	0.278	68.9	132.2

CA: contact angle (º).

Table 5
Results of the ANOVA.

Process parameter	DOF	Sum of squares	Variance	Contribution Percent
T_h (ºC)	2	50.322	25.161	60.854
Q_h (mL/min)	2	8.053	4.026	9.739
C_i (kg/m^3)	2	12.138	6.069	14.679
Q_s (Nm^3/h)	2	12.177	6.088	14.726
Other/Error	0	0.00164	0.0008	0.002
Total	8	82.69164	-	100.00%

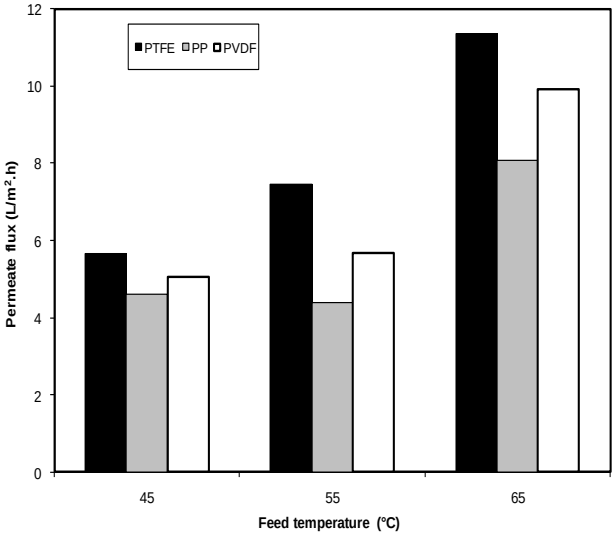

Fig.4. Main effects of feed temperature on the permeate flux for the investigated membranes (PTFE, PP and PVDF, all 0.22 µm).

3.2. Main effects of feed flow rate

If only a non-volatile solute is presented in the feed (as the subject of this work or in case of desalination), during SGMD process the solute concentration (i.e. glucose concentration in this case) at the feed-membrane interface becomes greater than that of the feed bulk. This can result in decreasing the permeate flux. This is the effect of concentration polarization phenomenon. However, for feed stream containing volatile chemicals, such as ethanol [17], the temperature polarization effect is more influence than that of the concentration polarization effect.

On the other hand, like other membrane separation processes [36,37], SGMD process is also sensitive to fouling phenomenon. Moreover, the non-isothermal characteristics of SGMD process can lead to temperature polarization [38]. Both polarizations and membrane fouling decrease the permeate flux due to the formation of concentration and temperature boundary layers, which can impose mass and temperature resistant layers against the transfer of vapor molecules through the open pores of the applied membrane [27]. These shortcomings may be overcome by promoting the hydraulic characterization such as increasing the flow velocity, using turbulence promoters, breaking the boundary layer or using pulsation flow at the membrane-fluid interface. Among the proposed strategies, decreasing the effect of polarizations' effects through Reynolds number variation (variation of superficial velocity in the membrane-feed interface) can be investigated as one of the simplest methods [39].

Figure 5 shows the influence of the flow rate in the feed channel on the permeate flux. As can be seen, the increase in the feed flow rate from 400 to 600 mL/min promoted the permeate flux due to slightly improvement in the fluid turbulency at the membrane-feed interface. It is to be noted that in the proposed flow range (400 to 600 mL/min), the higher feed flow rate is positive for all three investigated membranes, however, it was more effective for the PTFE one. A small decrease in permeate flux was observed when the flow rate was increased from 600 to 800 mL/min which can be attributed to an increase in overall heat transfer coefficient at higher flow rates. This also decreases the temperature gradient across the membrane. In addition, using higher inlet flow rates can be translated into the necessity of applying higher pressure in the feed channel. This increases the pore wetting risk, as well (i.e. the most important weak point of the MD process). Moreover, in a recent modeling study on the membrane pore wetting in VMD process, it was discussed that intrusion of the process liquid into the pores (i.e. partial pore wetting) may cause severe temperature polarization inside the pore reducing the permeate flux. It should be noted that in the case of partial pore wetting, there is no feed leakage from the feed channel to the permeate channel and therefore the selectivity is remained high yet. Therefore, increasing the flow rate in the feed channel can reduce temperature polarization on the membrane surface and increases the permeate flux, as well.

On the other hand, increasing the flow rate can increase the possibility of partial pore wetting and consequently cause the reduction in the permeate flux. Hence, there should be an optimal point for permeate flux by changing the flow rate. Therefore, the reduction in flux for the highest flow rate might be due to the partial pore wetting, too [40]. However, further studies should be carried out to comprehensive understanding the influence of the feed flow on the permeate flux in the SGMD process. Moreover, fabrication of next generation of membranes with higher hydrophobicity and surface features, as well as enhanced performance for polarization effects, mass transfer and thermal efficiency would be acknowledged as a promising solution for using higher feed velocity in MD process toward progressing the permeate flux [41,42].

Moreover, the increase in the feed flow rate was more effective for the PTFE membrane as compared with the PP and the PVDF membranes. The reason behind the better performance of the PTFE membrane is discussed in the following sections (*3.5*).

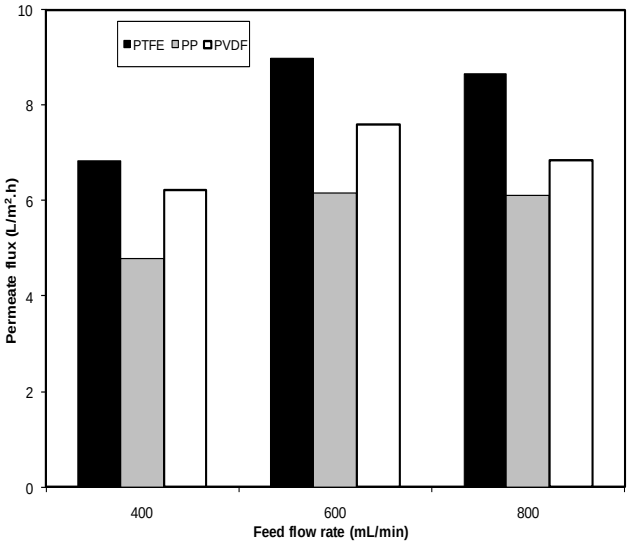

Fig. 5. Main effects of feed flow rate on the permeation flux.

this can be concluded that the effect of the gas boundary layer in the SGMD process is more significant and effective than that of the liquid boundary layer in the feed channel (hot side). This was also confirmed experimental by Khayet and co-workers which the heat transfer coefficient in the liquid phase is much larger than that of the gas phase (permeate channel) [47,48].

As could be observed in Figure 7, considerably higher permeate flux obtained for the PTFE membrane by using higher gas flow rate in the permeate channel in comparison with the PP and PVDF membranes. An increase in the gas flow rate (0.113 to 0.283 Nm3/h) showed a negligible effect on the permeate flux of the PP membrane. A slight reduction was observed for the PVDF membrane in the same gas flow rate range. This result can be ascribed to the structure of these membranes. However, further studies should be carried out to make this result clear.

Furthermore, the permeate flux was increased by progressing the sweeping gas flow rate from 0.283 to 0.453 Nm^3/h, and this trend was observed for all used membranes. This can be explained by the fact that an increase in the gas flow rate (or its superficial velocity in the permeate channel) leads to an increase in the vacuum situation at the pore's entrance point (in the permeate channel). Consequently, higher mass transfer coefficients help to provide a greater driving force and higher permeate flux, as well. Moreover, as can be seen (see Figure 7), the applied membranes had various performances at the same operating conditions. Such behavior can be attributed to their different structural characteristics, i.e. the morphology and topography, which is discussed in the next section.

3.3. Main effects of feed concentration

As can be seen in Figure 6, imposing higher glucose concentration to feed stream (10 to 50 kg/m^3) reduced the permeate flux for all the used membranes. This can be attributed to the lower water activity in the feed stream. It is to be noted that in the SGMD process, the influence of temperature polarization is more significant as compared with the concentration polarization effect. However, as mentioned earlier one of the highlighted advantages of the SGMD process is that this non-isothermal separation process is not influenced by osmotic pressure. This is in contrast to RO which suffers from the osmotic pressure of the feed) and is less sensitive to the feed concentration. This can be explained as follow.

Outdoor condensation of the permeated vapor molecules in the SGMD process needs an external condenser to collect the produced fresh water. This can lead to more complication of the SGMD system as well as increasing the overall costs. Consequently, the SGMD process seems to be more promising for the processes in which the permeate stream is not the main product. For instance, feed stream containing non-volatile solutes can be effectively processed by SGMD [24].

Moreover, as almost complete solute rejection can be achieved by MD (theoretically), highly concentrated solutions can be processed by the SGMD process. For instance, further treating the RO-reject stream using a hybrid MD-crystallization system is a promising option [43-45]. However, an increase in the feed concentration led to permeate flux decline. This can be attributed to both the lower vapor pressure (caused by reduction of water activity) and higher effect of the concentration polarization (as described in the section *3.2*). Moreover, the crystallization may also occur in the SGMD process when feed concentration performs above its saturation degree. However, the crystallization process, scale forming and fouling in SGMD process has not been studied yet and could be investigated as a promising subject for future studies in this field.

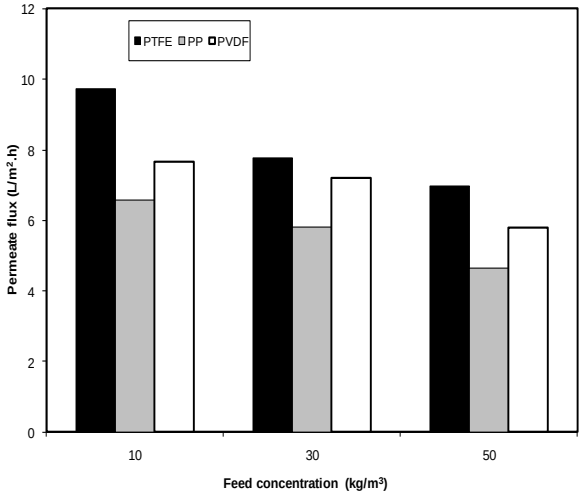

Fig. 6. Main effects of feed concentration on the permeation flux.

3.4. Main effect of sweeping gas flow rate

In the SGMD process, higher hydrostatic pressure should be used for the feed channel as compared with the permeate channel. The inlet pressure of the feed and the sweeping gas in the hot and cold channels remained at 0.30 and 0.25 bar, respectively. Based on the experimental results (see Figure 7), the sweeping gas flow rate significantly affects the permeate flux. Following explanations can support the obtained results.

Higher gas flow in the permeate channel can increase the Reynolds number. This can cause the change in the flow regime from the laminar to the transitional and then to the turbulent flow. Higher heat transfer coefficients in the permeate channel caused by turbulence gas flow can reduce the temperature polarization effect on the membrane surface in the permeate channel [46]. Therefore, the gas temperature at the membrane surface approaches that of the colder bulk gas stream. This can provide higher temperature difference and consequently higher vapor pressure difference (driving force), i.e. higher permeate flux. Based on the experimental results

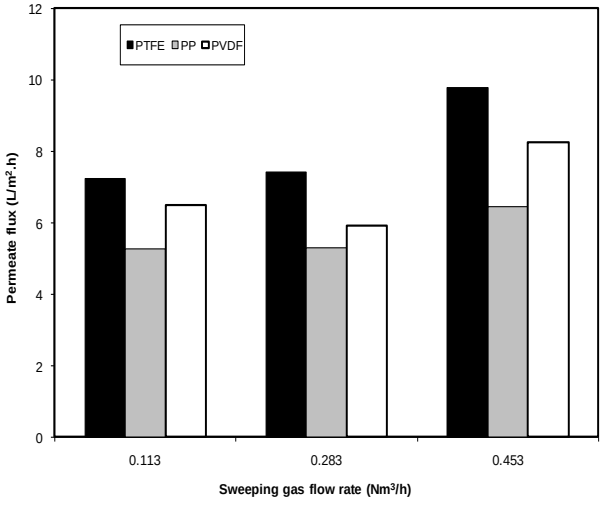

Fig. 7. Main effects of sweeping gas flow rate on the permeation flux.

3.5. Selectivity of the membranes

Pore wetting is a shortcoming and a serious bottleneck of MD processes. Therefore, in addition to the permeate flux, which was considered as the target parameter in this work, the selectivity of the process is also important; although, the theoretical selectivity of the SGMD process in the presence of compounds with very low vapor pressure in the feed stream can be almost 100% [30, 48].

A number of experimental runs were conducted under the constant operating conditions (T_h: 65°C, Q_h: 600 mL/min, C_f: 50 kg/m^3, and Q_c: 0.453 Nm^3/h) to examine the applied membranes in term of their selectivity. In these tests, the permeate samples were collected and examined for the glucose content. The results which have been presented in Figure 8 indicate that the SGMD process had very high selectivity, which is in good agreement with the theoretical basis of the MD process. Among the used membranes, the PVDF membrane showed the least selectivity, while the PTFE membrane had the highest glucose rejection, i.e. ~99.99%. This can be attributed to the higher hydrophobicity of the PTFE membrane as compared to other studied membranes (with 132±5° contact angle, see Table 4) among the other tested membranes. The higher the membrane hydrophobic is, the higher the higher the liquid entry pressure (LEP) is. It is worth quoting that the high LEP value is an essential specifications required for MD membranes. Moreover, this result is in good agreement with the results of previous studies [13, 15, 49], which indicated when an applied membrane for an MD application should be selected among those commercially available MF membranes, the PTFE membrane is bold, regardless what the feed type is.

Further to hydrophobicity, other membrane characteristics such as pore size and its distribution, thickness, porosity and surface roughness can significantly influence the MD membrane performance, i.e. selectivity and permeate flux. These specifications can be obtained by the morphological and the topographical studies of the applied membranes, via SEM and AFM observations, respectively. Figure 3 presents the SEM monographs and AFM images of the studied membranes in this work.

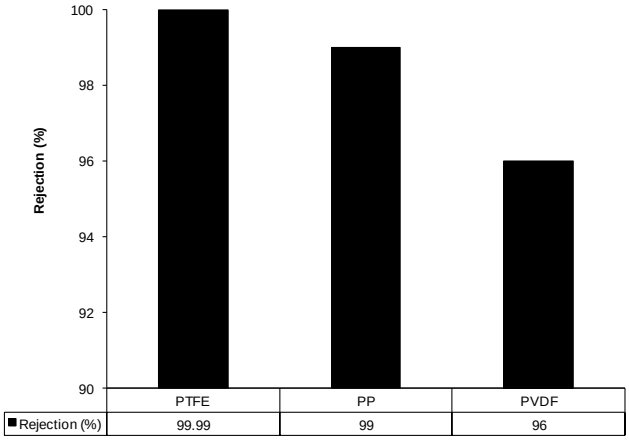

Fig. 8. Glucose rejection values of the membranes. (T_h = 65°C, Q_h = 600 mL/min, C_i = 50 kg/m^3 and Q_s = 0.453 Nm^3/h).

The membrane pore size and its distribution are two crucial features for a proper SGMD performance by avoiding the liquid penetration into the pores. Therefore, due to the nature of the driving force in SGMD process, which is the vapor pressure difference, only vapor molecules should be presented in the membrane pores and corresponding channels. According to the published results in the literature, the optimum pore size range for an MD membrane is approximately between 0.1 to 0.45 µm [49-52]. However, it should be noted that the real value for the membrane' pore size and those reported by the supplier can be different. This is due to various fabrication methods for membrane preparation by manufacturers. As a result, in MD applications, which the pore size has a critical role, it would be better to characterize this item (pore size and its distribution) before using in SGMD process. Various techniques have been used to measure these parameters [53]. Among them, topography observation using atomic force microscopy (AFM) has been recently attracted considerable attention [54]. In this work, the membranes with 0.22 µm pore size were characterized using AFM method.

Table 4 presents both reported and characterized values for pore size and roughness parameters for polymer membranes. The reported value of mean pore size for all membranes is 0.2 µm by supplier. However, this parameter was measured differently for proposed membranes: 0.287, 0.311 and 0.282 µm for PTFE, PVDF and PP membranes, respectively. The pore size distribution of the studied membranes is shown in Figure 9. The pore size distribution of the studied membranes was measured as described elsewhere [27]. As could be observed, the PTFE membrane had the narrowest post size distribution. In case of PTFE membrane, about 47% of the measured pores were in the range of 0.25 µm. This value is quite close to the reported one by the supplier. The sharpness in the pore size distribution graph is in the order of PTFE > PP > PVDF. A wider pore size distribution was observed for the PVDF membrane as compared to other membrane.

On the other hand, the PTFE membrane is rougher and the more hydrophobic as compared with others membranes. It can be concluded that that rougher surface not only increase the hydrophobicity, but also can increase the micro-mixing effect in the feed-membrane interface resulting in reduction the negative effect of polarization effects on the permeate flux.

Therefore, lower permeate flux and solute rejection of PVDF membrane can be attributed to its weaker characteristics, i.e. larger pore size and wider pore size distribution, as well as lower hydrophobicity. In contrast to PVDF and PP membranes, the higher obtained permeate flux and solute rejection of PTFE membrane can be attributed to its rougher (68.9 nm) and higher contact angle (~132°), as well as narrower pore size and its distribution. Therefore, based on the obtained results, PTFE membrane was used for next experiments.

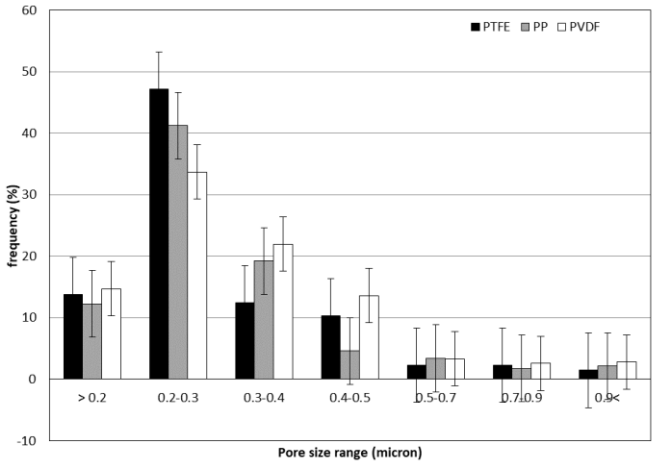

Fig. 9. Pore size distribution of applied membranes analysed by AFM method. (PTFE, PP and PVDF with 0.22 µm reported pore size).

3.6. The analysis of variance (ANOVA)

Table 5 shows ANOVA results (the analysis of variance) for PTFE membrane. The ANOVA results indicate that T_h, Q_s and C_i are the most important process parameters affecting the permeate flux. T_h was registered as the most significant parameter (the highest contribution: 60.854%) and Q_h showed the lowest effect on the permeate flux (contribution: 9.739%). Higher impact of the feed temperature (T_h) can be attributed to the nature of the SGMD process, which is a non-isothermal separation process [55,56]. Higher evaporation efficiency for water molecules can be expected (due to the exponential increase of vapor pressure) when higher operating temperature is imposed to the feed solution. However, this can reasonably be lower than that of the boiling temperature. Consequently, this results in higher permeate flux.

Another conclusion in this work is that, due to the module configuration in SGMD process, where the active side of the membrane is in direct contact with the hotter process liquid and the backing side is in direct contact with the colder sweeping gas flow, the temperature polarization is located in the permeate channel. This is in good agreement with the results of previous works in the literature [57,58]. That is why even a small change in the gas flow rate can considerably change the permeate flux of SGMD process, in contrast of the feed flow rate.

Based on the Taguchi model prediction, the optimum condition for

SGMD process in this work is:

$$A_3B_2C_1D_3 \quad (1)$$

where A_3 represents 65°C, B_2 represents 600 mL/min, C_1 represents 10 kg/m^3 and D_3 represents 0.453 Nm^3/h. Based on the proposed operating conditions, the predicted permeate flux is 15.388 L/m^2.h. Therefore, an experimental run was performed in order to confirm the prediction of the Taguchi model. The experimental permeate flux by using the proposed operating conditions ($A_3B_2C_1D_3$) was measured at 15.43 L/m^2.h with an error value of <0.3%.

3.7. Effect of flow arrangements in the SGMD module on the permeation flux

As mentioned earlier, SGMD process involves simultaneous mass and heat transfers. Module design and flow arrangement, therefore, are important factors governing the efficiency of the MD processes [59,60]. However, module design for the SGMD process has not yet been addressed comprehensively. Therefore, the flow arrangement inside the SGMD module was investigated as an effective parameter. Three flow arrangements were studied including co-current, counter-current and cross-current flow patterns (see Figure 2). The obtained results is shown in Figure 10. As could be observed, the counter-current flow arrangement resulted in higher permeate flux than that of the co-current flow. A good agreement was observed with the previously published work in the literature [60].

In this work, a new flow arrangement inside the SGMD module was developed for the first time which is cross-current flow. Based on the obtained results, higher permeate flux was achieved by imposing the new flow arrangement inside the SGMD module (cross-current), under the same operating conditions, as compared with the two other conventional flow arrangements (see Figure 10). This achievement can be explained as follow.

When the co-current configuration is used, the maximum driving force is registered for the entrance zones of the SGMD module. This driving force is obviously higher than that of the registered value for the counter-current configuration. However, this the vapor pressure difference (ΔP) decreases along the membrane module. The value for ΔP can even approach to zero for long length of the SGMD module. This is due to the considerable reduction in temperature difference (ΔT) in this flow arrangement (co-current). Opposed to it, a constant driving force can be observed for the counter-current configuration. In better words, lower and higher driving forces can be achieved in at the entrance and exit zones of the SGMD module by imposing the counter-current flow arrangement as compared with the co-current one. Therefore, it can be resulted that the system does not approach to the equilibrium state in the counter-current flow arrangement due to higher overall driving force. This is in good agreement with the published results in literature [59,60].

The cross-flow configuration for SGMD module, however, is even more efficient than both the co-current and the counter-current ones (see Figure 10). This configuration works like baffled heat-exchangers. In this structure, the counter-current flow can be changed to the more efficient cross-flow configuration by imposing the baffles. As a result, higher ΔT and consequently higher ΔP can be provided inside the module, as compared with the co-current and counter-current configurations. This then results in overall improvement of the thermally-driven mass transfer and the higher permeate flux in SGMD process. Moreover, this new flow arrangement (i.e. cross-flow) not only can be effectively used for SGMD configuration, but also it found as an efficient configuration for DCMD process, as it discussed comprehensively in our previous work [19].

As the both side of the used membrane is in direct contact with process fluids in SGMD module, the superficial velocities in the feed and permeate channels can be investigated as effective parameters for enhancing the permeate flux. The superficial velocity is then a function of channels depth, even if the flow rate remains constant. As could be observed in Figures11, by increasing the flow channels depth (for both the feed and the permeate streams) from 2 mm to 6 mm, the permeate flux decreased, significantly. This can be reasonable because by increasing the flow channel depth, the superficial velocity decreases and consequently, both concentration and temperature polarization effects increase. However, further studies are needed in this case.

4. Conclusions

We successfully examined SGMD process for concentrating of glucose syrup with different concentrations. This is a critical stage in food industry and bioethanol production. Based on the obtained results, it can be concluded that the importance order of the operating parameters for achieving the highest permeate flux and rejection is: T_h (feed temperature) > Q_s (gas flow rate) > C_i (feed concentration) > Q_h (feed flow rate).

In addition to process parameters, the physical features of the used membrane; including pore size and its distribution, as well as the surface hydrophobicity are also important.

The module design was found crucial in case of the flow arrangement and the cross-current configuration can enhance the permeate flux progressively. This is due to provide higher driving force by using this configuration.

Based on the obtained results, it can be concluded that PTFE membrane with a 0.22 µm pore size exhibited the best performance for concentrating of glucose syrup.

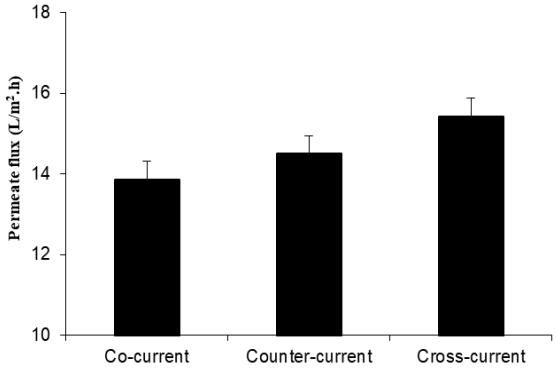

Fig. 10. Effect of flow arrangement inside the membrane module on the permeation flux (T_h = 65°C, Q_h = 600 mL/min, C_i = 10 kg/m^3 and Q_s = 0.453 Nm^3/h).

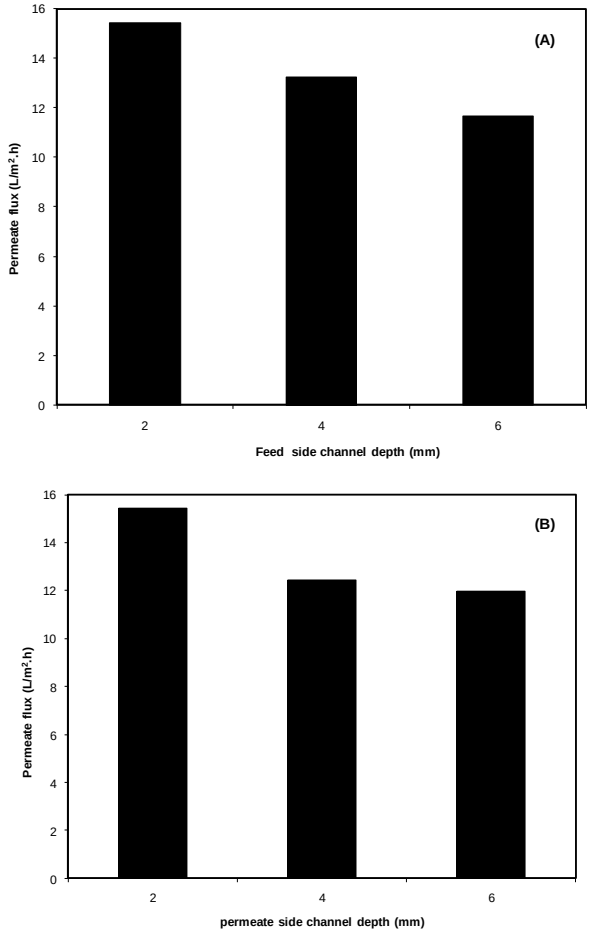

Fig. 11. Effect of the module depth in the hot side (A) and permeate side (B) on the permeation flux (T_h =65°C, Q_h =600 mL/min, C_i =10 kg/m^3 and Qs =0.453 Nm^3/h).

References

[1] J. Zuo, J.Y. Lai, T.S. Chung, In-situ synthesis and cross-linking of polyamide thin film composite (TFC) membranes for bioethanol applications, J. Membr. Sci. 458 (2014) 47-57.

[2] A. Noureddin, M.M.A. Shirazi, J. Tofeily, P. Kazemi, E. Motaee, A. Kargari, M. Mostafaei, M. Akia, T. Hamieh, M. Tabatabaei, Accelerated decantation of biodiesel-glycerol mixtures: Optimization of a critical stage in biodiesel biorefinery, Sep. Purif. Technol. 132 (2014) 272-280.

[3] K. Li, S. Liu, X. Liu, An overview of algae bioethanol production, Int. J. Energy Res. 38 (2014) 965-977.

[4] R. Koppram, E. Tomas-Pejo, C. Xiros, L. Olsson, Lignocellulosic ethanol production at high-gravity: challenges and perspectives, Trends Biotechnol. 32 (2014) 46-53.

[5] P. Peng, B. Shi, Y. Lan, A review of membrane materials for ethanol recovery by pervaporation, Sep. Sci. Technol. 46 (2010) 234-246.

[6] B. Van der Bruggen, P. Luis, Pervaporation as a tool in chemical engineering: a new era?, Current Opinion Chem. Eng. 4 (2014) 47-53.

[7] L.M. Vane, A review of pervaporation for product recovery from biomass fermentation processes, J. Chem. Technol. Biotechnol. 80 (2005) 603-629.

[8] S.N. Naik, V.V. Goud, P.K. Rout, A.K. Dalai, Production of first and second generation biofuels: A comprehensive review, Renew. Sustain. Energy Rev. 14 (2010) 578-597.

[9] Y. He, D.M. Bagley, K.T. Leung, S.N. Liss, B.Q. Liao, Recent advances in membrane technologies for biorefining and bioenergy production, Biotechnology Adv 30 (2012) 817-858.

[10] P. Wei, L.H. Cheng, L. Zhang, X.H. Xu, H.I. Chen, C.J. Gao, Areview of membrane technology for bioethanol production, Renew. Sustain. Energy Rev. 30 (2014) 388-400.

[11] S.S. Madaeni, S. Zereshki, Reverse osmosis: an energy saving option in sugar industry, Desalination 200 (2006) 374-375.

[12] S.S. Madaeni, S. Zereshki, Energy consumption for sugar manufacturing. Part I: Evaporation versus reverse osmosis, Energy Conv. Manage. 51 (2010) 1270-1276.

[13] M.M.A. Shirazi, A. Kargari, A review on application of membrane distillation (MD) process for wastewater treatment, J. Membr. Sci. Res, 1 (2015) 101-112.

[14] H. Susanto, Towards practical implementations of membrane distillation, Chem. Eng. Process 50 (2011) 139-150.

[15] M. Khayet, Membranes and theoretical modeling of membrane distillation: A review, Adv. Colloid Interf. Sci. 164 (2011) 56-88.

[16] A. Alkhudhiri, N. Darwish, N. Hilal, Membrane distillation: A comprehensive review, Desalination 287 (2012) 2-18.

[17] M.M.A. Shirazi, A. Kargari, M. Tabatabaei, Sweeping gas membrane distillation (SGMD) as an alternative for integration of bioethanol processing: study on a commercial membrane and operating parameters, Chem. Eng. Communic. 202 (2014) 457-466.

[18] M. Sohrabi, A. Kargari, Modeling and application of UF-stirred cell reactors in hydrolysis of saccharides, Chem Eng Technol 22 (1999) 955-962.

[19] M.M.A. Shirazi, A. Kargari, M. Tabatabaei, Evaluation of commercial PTFE membranes in desalination by direct contact membrane distillation, Chem. Eng. Proc.: Process Intensif. 76 (2014) 16-25.

[20] M.M.A. Shirazi, D. Bastani, A. Kargari, M. Tabatabaei, Characterization of polymeric membranes for membrane distillation using atomic force microscopy, Desal. Water Treat. 51 (2013) 6003-6008.

[21] M.M.A. Shirazi, A. Kargari, S. Bazgir, M. Tabatabaei, M.J.A. Shirazi, M.S. Abdullah, T. Matsuura, A.F. Ismail, Characterization of electrospun polystyrene membrane for treatment of biodiesel's water-washing effluent using atomic force microscopy, Desalination 329 (2013) 1-8.

[22] M.M.A. Shirazi, A. Kargari, M. Tabatabaei, A.F. Ismail, T. Matsuura, Assessment of atomic force microscopy for characterization of PTFE membranes for membrane distillation (MD) process, Desal. Water Treat. 54 (2014) 295-304.

[23] A. Kargari, T. Kaghazchi, M. Soleimani, Role of emulsifier in the extraction of gold (III) ions from aqueous solutions using the emulsion liquid membrane technique, Desalination 162 (2004) 237-247.

[24] M.M.A. Shirazi, A. Kargari, M. Tabatabaei, A.F. Ismail, T. Matsuura, Concentration of glycerol from dilute glycerol wastewater using sweeping gas membrane distillation, Chem. Eng. Proc.: Process Intensif. 78 (2014) 58-66.

[25] T. Mohammadi, P. Kazemi, Taguchi optimization approach for phenolic wastewater treatment by vacuum membrane distillation, Desal. Water Treat. 52 (2014) 1341-1349.

[26] M.A. Izquierdo-Gil, J. Abildskov, G. Jonsson, The use of VMD data/model to test different thermodynamic models for vapor-liquid equilibrium, J. Membr. Sci. 239 (2004) 227-241.

[27] M. Khayet, T. Matsuura, Membrane distillation: Principles and applications, ELSEVIER, 2011.

[28] L. Eykens, I. Hitsov, K. De Sitter, C. Dotremont, L. Pinoy, I. Nopens, B. Van der Bruggen, Influence of membrane thickness and process conditions on direct contact membrane distillation at different salinities, J. Membr. Sci. 498 (2016) 353-364.

[29] L. Eykens, K. De Sitter, C. Dotremont, L. Pinoy, B. Van der Bruggen, Characterization and performance evaluation of commercially available hydrophobic membranes for direct contact membrane distillation, Desalination 392 (2016) 63-73.

[30] M. Khayet, P. Godino, J.I. Mengual, Theoretical and experimental studies on desalination using the sweeping gas membrane distillation method, Desalination 157 (2003) 297-305.

[31] T. Vazirnejad, J. Karimi-Sabet, A. Dastbaz, M.A. Moosavian, S.A. Ghorbanian, Application of salt additives and response surface methodology for optimization of PVDF hollow fiber membrane in DCMD and AGMD processes, J. Membr. Sci. Res. 2 (2016) 169-178.

[32] N.S. Mohd Yatim, K. Abd. Karim, O. Boon Seng, Performance of chemically modified TiO2-poly(vinyllidene fluoride) DCMD for nutrient isolation and its antifouling properties, J. Membr. Sci. Res. 2 (2016) 163-168.

[33] A. Kargari, M.M.A. Shirazi, Water desalination: Solar-assisted membrane distillation, in: Encyclopedia of Energy Engineering and Technology (2nd Ed.), Taylor & Francis, (2014) DOI: 10.1081/E-E.

[34] Sh. Gorjian, B. Ghobadian, Solar desalination: A sustainable solution to water crisis in Iran, Renew. Sustain. Energy Rev. 48 (2015) 571-584.

[35] O. Nematollahi, H. Hoghooghi, M. Rasti, A. Sedaghat, Energy demands and renewable energy resources in the Middle East, Renew. Sustain. Energy Rev. 54 (2016) 1172-1181.

[36] S. Shirazi, C.J. Lin, D. Chen, Inorganic fouling of pressure-driven membrane processes-A critical review, Desalination 250 (2010) 236-248.

[37] W. Guo, H.H. Ngo, J. Li, A mini-review on membrane fouling, Bioresource Technol. 122 (2012) 27-34.

[38] M. Khayet, P. Godino, J.I. Mengual, Thermal boundary layers in sweeping gas membrane distillation processes, AIChE J. 48 (2002) 1488-1497.

[39] M.M.A. Shirazi, A. Kargari, A.F. Ismail, T. Matsuura, Computational fluid dynamic (CFD) opportunities applied to the membrane distillation process: State-of-the-art and perspectives, Desalination 377 (2016) 73-90.

[40] L. Francis, N. Ghaffour, A.S. Alsaadi, S.P. Nunes, G.L. Amy, Performance evaluation of the DCMD desalination process under bench scale and large scale module operation conditions, J. Membr. Sci. 455 (2014) 103-112.

[41] E. Guillen-Burrieza, A. Servi, B.S. Lalia, H.A. Arafat, Membrane structure and surface morphology impact on the wetting of MD membranes, J. Membr. Sci. 483 (2015) 94-103.

[42] Sh. Tabe, A review of electrospun nanofiber membranes, J. Membr. Sci. Res. 3 (2017) 228-239.

[43] X. Ji, E. Curcio, S. Al Obaidani, G. Di Profio, E. Fantananova, E. Drioli, Membrane distillation-crystallization of seawter reverse osmosis brines, Sep. Purif. Technol. 71 (2010) 76-82.

[44] J. Kim, J. Kim, S. Hong, Recovery of water and minerals from shale gas produced water by membrane distillation crystallization, Water Res. 129 (2018) 447-459.

[45] A. Ali, C.A. Quist-Jensen, E. Drioli, F. Macedonio, Evaluation of integrated microfiltration and membrane distillation/crystallization processes for produced water treatment, Desalination434 (2018) 161-168.

[46] M. Asghari, M. Dehghani, H.R. Harami, A.H. Mohammadi, Effects of operating parameters in sweeping gas membrane distillation process: Numerical simulation of Persian Gulf seawater desalination, J. Water Environ. Nanotech. 3 (2018) 128-140.

[47] M. Khayet, P. Godino, J.I. Mengual, Nature of the flow on sweeping gas membrane distillation, J. Membr. Sci. 170 (2000) 243-255.

[48] M. Khayet, P. Godino, J.I. Mengual, Theory and experiments on sweeping gas membrane distillation, J. Membr. Sci. 165 (2000) 261-272.

[49] M.M.A. Shirazi, A. Kargari, M.J.A. Shirazi, Direct contact membrane distillation for seawater desalination, Desal. Water Treat. 49 (2012) 368-375.

[50] A. Criscuoli, J. Zhong, A. Figoli, M.C. Carnevale, R. Huang, E. Drioli, Treatment of dye solutions by vacuum membrane distillation, Water Res. 42 (2008) 5031-5037.

[51] K.J. Lu, Y. Chen, T.S. Chung, Design of omniphobic interfaces for membrane distillation – A review, Water Res. 162 (2019) 64-77.

[52] L.N. Nthunya, L. Gutierrez, S. Derese, E.N. Nxumalo, A.R. Verliefde, B.B. Mamba, S.D. Mhlanga, A review of nanoparticle-enhanced membrane distillation membranes: membrane synthesis and applications in water treatment, J. Chem. Technol. Biotechnol. 94 (2019) 2757-2771.

[53] C. Zhao, X. Zhou, Y. Yue, Determination of pore size and pore size distribution on the surface of hollow-fiber filtration membranes: a review of methods, Desalination 129 (2000) 107-123.

[54] M. Khayet, K.C. Khulbe, T. Matsuura, Characterization of membranes for membrane distillation by atomic force microscopy and estimation of their water vapor transfer coefficients in vacuum membrane distillation process, J. Membr. Sci. 238 (2004) 199-211.

[55] L. Fatehi, A. Kargari, D. Bastani, M. Soleimani, M.M.A. Shirazi, Saline brine desalination: application of sweeping gas membrane distillation (SGMD), Desal. Water Treat. 71 (2017) 12-18.

[56] V. Perfilov, V. Fila, J. Sanchez Marcano, A general predictive model for sweeping gas membrane distillation, Desalination 443 (2018) 285-306.
[57] M.M.A. Shirazi, A. Kargari, Concentrating of sugar syrup in bioethanol production using sweeping gas membrane distillation, Membranes 9 (2019) 59. https://doi.org/10.3390/membranes9050059.
[58] S.E. Moore, S.D. Mirchandani, V. Karanikola, T.M. Nenoff, R.G. Arnold, A.E. Saez, Process modeling for economic optimization of a solar driven sweeping gas membrane distillation desalination system, Desalination 437 (2018) 108-120.
[59] A. Kargari, M.M.A. Shirazi, Application of membrane separation technology for oil and gas produced water treatment, in: Advances in Petroleum Engineering (vol. 1), Studium Press LLC, USA, 2014.
[60] K. He, H.J. Hwang, M.W. Woo, I.S. Moon, Production of drinking water from saline water by direct contact membrane distillation (DCMD), Ind. Eng. Chem. Res. 17 (2011) 41-48.